

Establishing a Mechanical Homeostatic State in the Cardiac System to Study Growth and Remodeling of the Myocardial Tissue

Teresa Díaz Jordá^{1*}, Shaiv Parikh^{1*}, Martin R. Pfaller², Marcos Latorre¹

¹ Center for Research and Innovation in Bioengineering, Universitat Politècnica de València, Spain

² Department of Biomedical Engineering, Yale University, New Haven, USA

**Equal contribution*

Abstract

Determining the deposition pre-stretch of elastin is a critical challenge for initializing growth and remodeling (G&R) simulations in soft tissues, as it is essential for defining mechanical homeostasis. We developed a two-stage implementation to numerically determine the stress-free configuration of elastin in cardiac tissue. Firstly, assuming a balance between body forces from tissue constituents and traction forces in equilibrium, the forces experienced by the elastin are obtained. Secondly, a forward iterative algorithm was implemented to determine the stress-free state of elastin. The method was validated with a cylindrical geometry against an analytical solution. Lastly, the stress-free state of elastin was obtained for an idealized left ventricle model, which shows the applicability of this framework to enable future mechanistic G&R studies on cardiac tissue.

1. Introduction

Growth and remodeling (G&R) in soft tissue can be triggered by a loading or structural perturbation of its homeostatic state [1]. Constrained mixture models (CMMs) are a mathematical framework in which the G&R of soft tissues is modelled as the evolution of a composite material where structurally significant constituents, each with their own stress-free state and turnover rate, are constrained to a common loaded configuration, while mechanical equilibrium is maintained at tissue-level. CMMs use the loaded *in vivo* state as the reference configuration, which requires defining a deposition stretch for each constituent. This parameter quantifies the stretch from a constituent's natural, stress-free state to its incorporated state in the loaded tissue. In mechanical equilibrium, load-bearing constituents also satisfy mechanical homeostasis which is defined by the constituents found at a preferred deposition stretch. However, this requirement is particularly critical for constituents with extremely low turnover, such as elastin. Deposited during development with a half-life of decades, the elastin network maintains

its original deposition stretch [1]. This pre-stretch contributes as a pre-stress to the tissue that other constituents must balance as they are turnover. For collagen and muscle cells, some values of pre-stretch have been inferred computationally from ex-vivo experimental data of vascular [2] and myocardial tissue [3]. However, quantifying elastin's pre-stretch remains a challenging inverse problem. Computational inverse methods have been previously applied to estimate the stress-free reference configuration at tissue-level [4,5] as well as specifically for elastin [6]. These methods can be broadly categorized by their fundamental approach. For instance, the Backward Incremental Method [5] aims to find the reverse deformation path from the *in vivo* configuration by incrementally applying forward deformations to reconstruct the stress-free configuration. In contrast, forward methods like the Augmented Iterative Method [4] are optimization-based, as they iteratively run standard forward simulations, progressively updating the guess of a stress-free configuration until the resulting deformed state matches the known loaded configuration within a specified tolerance. The former approach involves more complex implementation, as it often demands substantial modifications to the numerical solver to formulate the inverse problem. In contrast, forward methods can leverage standard finite element solvers in a straightforward manner, without fundamental alterations to their core code.

Our goal is to develop a forward method to determine the stress-free configuration of elastin that will allow initialization of CMMs G&R simulations ensuring mechanical homeostasis.

2. Methods

We introduce a two-stage computational framework to numerically estimate the stress-free configuration of elastin. This computational pipeline was implemented using GIBBON MATLAB library [7] and the finite element (FE) solver FEBio [8].

2.1. Stage 1: Force balance in equilibrium

We assume that the current deformed configuration of a biological organ (Ω) is subjected to traction (\mathbf{t}) on boundary $\partial\Omega_t$. The balance of linear momentum yields that in all positions of this configuration the condition $\nabla \cdot (\boldsymbol{\sigma}_e(\mathbf{G}_e) + \boldsymbol{\sigma}_c(\mathbf{G}_c) + \boldsymbol{\sigma}_m(\mathbf{G}_m)) = \mathbf{0}$ is satisfied, where $\boldsymbol{\sigma}$ are the Cauchy stresses of the load-bearing constituents elastin (e), collagen (c) and muscle cells (m) that arise from the deposition stretch tensor $\mathbf{G}_i = \partial\mathbf{x}/\partial\mathbf{X}_i$, which represents the deformation of each constituent from its natural configuration ($\mathbf{X}_\alpha \in \Omega_{0,\alpha}$) to the current homeostatic state ($\mathbf{x} \in \Omega$). For fibrous constituents such as collagen and muscle cells, we prescribe homeostatic stretches λ_h^i and fiber directions \mathbf{a}_0^i (i = collagen, muscle cells) and the deposition stretch tensor as in Equation 1.

$$\mathbf{G}_i = \lambda_h^i \mathbf{a}_0^i \otimes \mathbf{a}_0^i + \frac{1}{\sqrt{\lambda_h^i}} (\mathbf{I} - \mathbf{a}_0^i \otimes \mathbf{a}_0^i) \quad (1)$$

Cauchy stresses $\boldsymbol{\sigma}_{collagen}$ and $\boldsymbol{\sigma}_{muscle}$ can thus be calculated and translated to forces as $\nabla \cdot \boldsymbol{\sigma}_i = \mathbf{f}_i$. The internal stresses of elastin remain unknown, but the linear momentum equation simplifies $\nabla \cdot (\boldsymbol{\sigma}_e) = -(\mathbf{f}_c + \mathbf{f}_m)$. In mechanical equilibrium, the internal forces must balance the traction forces on the boundary $\boldsymbol{\sigma} \cdot \mathbf{n} = \mathbf{t}$ which yields Equation 2.

$$\nabla \cdot (\boldsymbol{\sigma}_e) = \mathbf{t} - (\mathbf{f}_c + \mathbf{f}_m) \quad (2)$$

The traction forces result from the pressure (P_{ivo}) applied at the boundary of the tissue $\mathbf{t} = P_{ivo} \cdot \mathbf{n}$, where \mathbf{n} is a normal vector to the boundary (e.g., the arterial lumen or ventricular endocardium).

Thus, satisfying this relationship and the traction boundary condition, the only unknown to be determined is the pre-stretch of elastin, which is left to be determined in the second stage of the algorithm, once solved for the forces that are experienced by elastin as $\nabla \cdot (\boldsymbol{\sigma}_e) = \mathbf{f}_e$. These forces will depend on the prescribed in vivo pressure prescribed for traction forces, and prescribed fiber pre-stretches and orientations.

2.2. Stage 2: Prestressing algorithm

To determine the natural stress-free configuration of elastin Ω_0^e and ultimately determine elastin pre-stretches, we coupled our approach with the Augmented Iterative Method (AIM), previously described in the literature [4]. Briefly, the principle of this algorithm is to find a reference configuration (stress-free, Ω_0) so that, when subject to traction forces provided (\mathbf{f}_e), it deforms accordingly to approximate Ω_{ivo} . The AIM iteratively updates a reference configuration Ω_0^{k+1} by subtracting the per node displacement vector ($\mathcal{R}^k = \mathbf{x}^k - \mathbf{x}^{k+1}$) between

the updated deformed configuration Ω_k and the *in vivo* configuration, which is captured by a residual $\mathcal{R}^k = \|\mathbf{R}^k\|$. The algorithm stops when the residual falls below a defined tolerance ϵ ($= 10^{-3}$), while the number of iterations k is a result of this convergence. Thus, iteratively running forward finite element FE simulation \mathcal{S} expressed in Equation 3, providing net nodal forces \mathbf{f}_e we can obtain \mathbf{X}_e^k as the nodal coordinates for the stress-free elastin configuration Ω_0^e :

$$\mathbf{x}^k = \mathcal{S}((\mathbf{X}_e^k, \mathbf{0}), \text{net nodal forces}) \quad (3)$$

2.3. Analytical validation

A cylindrical geometry was considered to test the prestressing algorithm against an analytical solution of a stress-free configuration of elastin. We model an arterial segment as a cylinder (length $l = 2.50$ mm, inner diameter $r_i = 0.647$ mm, wall thickness $h = 0.04$ mm) discretized into 1860 linear hexahedral elements. Collagen homeostatic pre-stretch $\lambda_h^c = 1.10$ and a pressure of $P_{ivo} = 13.98$ kPa were prescribed. Only circumferential fibers were considered for simplification of the analytical resolution. Collagen energy strain function is modeled as in [1], with parameters $c_1^c = 235$ kPa, $c_2^c = 4.08$ kPa, and mass fraction $\phi_c = 0.33$, and the amorphous elastin matrix is modeled as a neo-Hookean material by means of a simplified hyperelastic Ogden model from with $c_1^e = 1600$ kPa, $c_2^e = 0$, $k_e = 4160$ kPa, $m_1 = 2$ and mass fraction $\phi_e = 0.67$. We apply Dirichlet boundary conditions to constrain the displacement in the circumferential ($\mathbf{u}(\mathbf{x})_{\theta=0} = \mathbf{0}$) and axial directions ($\mathbf{u}(\mathbf{x})_z = \mathbf{0}$) on one end of the cylinder.

2.3. Left Ventricle prestressing

We considered an idealized left ventricle (LV) mesh represented as a truncated ellipsoid (major epicardial radius $a_{epi} = 20$ mm, minor epicardial radius $b_{epi} = 10$ mm, and uniform wall thickness $h = 3$ mm) discretized into 900 linear hexahedra. We modeled both collagen and cardiomyocyte fibers as fiber-reinforced hyperelastic materials with a preferred fiber orientation as in [1]. Collagen follows the four-fiber family model with circumferential, axial and two diagonal ($\pm 45^\circ$) directions with material parameters $c_1^c = 234.9$ kPa, $c_2^c = 4.08$. Mass fractions for each collagen fiber direction as well as constituent mass fractions are equally distributed. Cardiomyocyte fibers follow a helix angle that varies continuously from $+60^\circ$ at the endocardium to -60° at the epicardium and its material parameters $c_1^m = 261.4$ kPa, $c_2^m = 0.24$. Similarly to the cylinder case, elastin is modeled as an Ogden neo-Hookean material with $c_1^e = 89.71$ kPa, $c_2^e = 0$, $k_e = 89.71 \cdot 10^3$ kPa, $m_1 = 2$. The fiber pre-stretches prescribed were $\lambda_h^c = 1.062$, and $\lambda_h^m =$

1.10. Material parameters were taken from vascular G&R model [1] and pre-stretches from [6]. Baseline systolic pressure of $16kPa$ ($= 120 mmHg$) was prescribed on the endocardium boundary to obtain elastin effective forces. The AIM ran applying fixed Dirichlet conditions on the nodes in the base in axial and circumferential directions ($\mathbf{u}(\mathbf{x})_\theta = \mathbf{0}$, $\mathbf{u}(\mathbf{x})_z = \mathbf{0}$; $\mathbf{x} \in \partial\Omega_{base}$).

3. Results and discussion

3.1. Cylinder case – Analytical solution

We assessed the agreement between our method and the analytical solution. In Figure 1, the two-stage implementation is depicted. Providing the forces \mathbf{f}_e obtained from the Stage 1, we contrasted our numerical solution for the inner radius (R_i) and thickness (H_i) of the undeformed configuration, given that analytically the circumferential stress in a thin wall cylinder can be expressed as $\sigma^\theta = P \cdot r_i / h$.

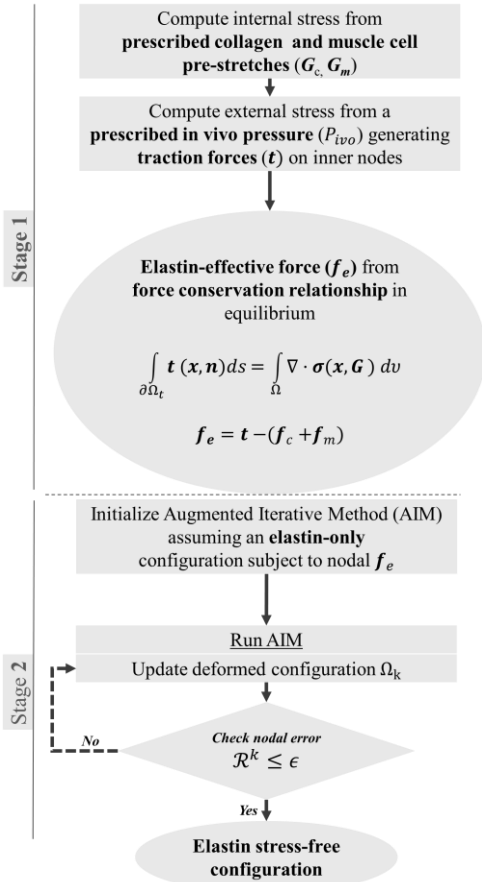


Figure 1. Flowchart for the two-stage implementation to find the stress-free configuration of elastin. In Stage 1, elastin effective forces are computed. In Stage 2, the AIM is run to find the stress-free configuration of elastin.

Numerically, we obtain that $R_i = 5.90 \cdot 10^{-1} mm$ and

$H_i = 4.16 \cdot 10^{-2} mm$, while the analytical ground truth values are $R_i^{GT} = 5.90 \cdot 10^{-1} mm$ and $H_i^{GT} = 4.17 \cdot 10^{-2} mm$, showing an exact match for the inner radius and a small relative error (0.24%) for the thickness. The agreement between our numerical results and the analytical solution shows the accuracy of the AIM implementation in solving the fundamental mechanobiological equilibrium problem.

3.3. Left ventricle prestress

The approach we provide can become useful to establish the stress-free state of elastin in tissues like myocardium, which is equally important to apply CMMs to study maladaptive G&R. We ran our implementation on an idealized LV as the *in vivo* geometry. It is worth noting that the material parameters used were taken from vascular G&R model developed in [1], while collagen and cardiomyocyte homeostatic pre-stretches were adopted from [6] which also were derived from vascular tissue, since CMM parameters for myocardium have not yet been inferred. In Figure 2, the stress-free configuration of elastin obtained with the AIM is shown.

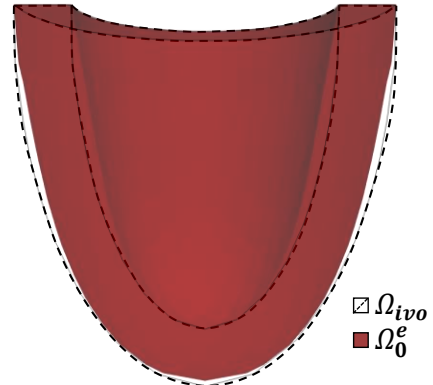


Figure 2. Cut view of the stress-free configuration of elastin (red) and in vivo LV geometry (dotted) obtained with the AIM implementation.

The convergence of the AIM is shown in Figure 3. After 8 iterations, a minimum residual $\mathcal{R}^k = 4 \cdot 10^{-4}$ was achieved, which is the minimum nodal difference between the original *in vivo* configuration and the updated *in vivo* geometry considering the resulting unstressed configuration of elastin subject to the effective forces obtained in the first stage of our implementation.

4. Limitations and future perspectives

This study has several limitations that provide a clear pathway for future research. Firstly, the material

parameters used were illustrative and not specifically calibrated to myocardial tissue, since these have not yet been characterized for CMMs. Hence, the presented results cannot be considered physiologically relevant but rather a proof of concept of a forward method. Secondly, the imposed Dirichlet boundary conditions on the base of the ventricle, while necessary for numerical stability, introduce artificial constraints that prevent a perfectly satisfied global force balance, potentially influencing the local stress field in the elements at the base. Employing alternative conditions like Robin-type boundaries in future studies could mitigate this issue. Additionally, comprehensive benchmarking against other established pre-stress algorithms using a wider range of material models will be essential for rigorously validating the method's robustness and performance, as well as initializing long-term growth and remodeling (G&R) simulations with the calculated homeostatic state. Finally, to fully establish this framework, future work will focus on applying the algorithm to realistic, patient-specific geometries derived from medical imaging.

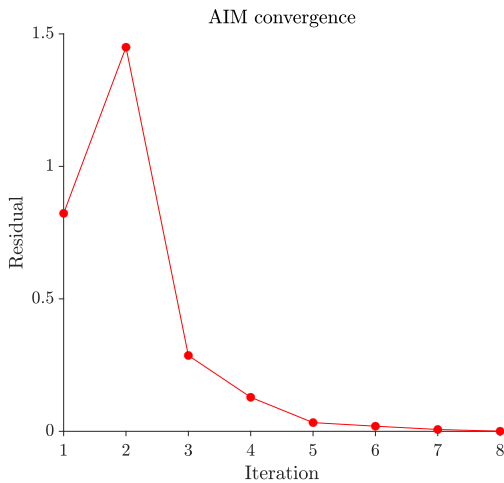


Figure 3. Augmented Iterative Method (AIM) convergence upon achieving minimum nodal error $\mathcal{R}^k \leq \epsilon$ for $\epsilon = 10^{-3}$.

5. Conclusions

By applying continuum mechanics principles, the developed framework infers the constituent-specific homeostatic forces that define mechanical equilibrium. The coupling of this principle with a forward iterative approach such as the AIM provides a robust methodology to estimate the stress-free configuration of elastin. We have tested our implementation by comparing our numerical solution with the known analytical solution for a thin-walled cylinder, showing perfect agreement between them. Unlike backward methods that require more complex implementations within the solver, the presented method should be easy to implement in any FE

solver as it only relies on iterative forward simulations until convergence is achieved. Our approach is directly applicable to left ventricular geometries to determine elastin's stress-free configuration that would enable further application of CMMs to study G&R in the cardiac tissue.

Acknowledgments

This work was supported by the European Union “Horizon Europe” research and innovation program (Grant Agreement 101039349 project G-CYBERHEART) and NIH R00HL161313.

References

- [1] Latorre M, Humphrey JD. Fast, rate-independent, finite element implementation of a 3D constrained mixture model of soft tissue growth and remodeling. *Computer Methods in Applied Mechanics and Engineering*. 2020 Aug 15;368.
- [2] Cardamone L, Valentín A, Eberth JF, Humphrey JD. Origin of axial pre-stretch and residual stress in arteries. *Biomechanics and Modeling in Mechanobiology*. 2009;8(6):431–46.
- [3] Grobbee MR, Shavik SM, Darios E, Watts SW, Lee LC, Rocca Bianca S. Contribution of left ventricular residual stress by myocytes and collagen: existence of inter-constituent mechanical interaction. *Biomechanics and Modeling in Mechanobiology*. 2018 Aug 1;17(4):985–99.
- [4] Rausch MK, Genet M, Humphrey JD. An augmented iterative method for identifying a stress-free reference configuration in image-based biomechanical modeling. *Journal of Biomechanics*. 2017 Jun 14;58:227–31.
- [5] Tziotziou A, Liu Y, Fontana F, Bierens J, Nederkoorn PJ, de Jong PA, et al. Pressure- and flow-driven biomechanical factors associate with carotid atherosclerosis assessed by computed tomography angiography. *Atherosclerosis*. 2025;
- [6] Gebauer AM, Pfaller MR, Braeu FA, Cyron CJ, Wall WA. A homogenized constrained mixture model of cardiac growth and remodeling: analyzing mechanobiological stability and reversal. *Biomechanics and Modeling in Mechanobiology*. 2023 Dec 1;22(6):1983–2002.
- [7] Moerman K. GIBBON: The Geometry and Image-Based Bioengineering add-On. *The Journal of Open Source Software*. 2018 Feb 19;3(22):506.
- [8] Maas SA, Ellis BJ, Ateshian GA, Weiss JA. FEBio: Finite Elements for Biomechanics. *Journal of Biomechanical Engineering*. 2012 Feb 9;134(1). Available from: <https://doi.org/10.1115/1.4005694>

Address for correspondence:

Teresa Díaz Jordá
Centro de Investigación e Innovación en Bioingeniería (Ci2B),
Universitat Politècnica de València (UPV), Valencia, Spain.
tediajor@upv.edu.es